

## Supporting Informations for

### Crystallization of Triple- and Quadruple-Stranded Dinuclear Bis- $\beta$ -diketonate-Dy(III)

#### Helicates: Single Molecule Magnet Behavior

Peng Chen,<sup>a</sup> Hongfeng Li,<sup>a</sup> Wenbin Sun,<sup>a</sup> Jinkui Tang,<sup>\*b</sup> Lei Zhang<sup>a</sup> and Pengfei Yan<sup>\*a</sup>

a. Key Laboratory of Functional Inorganic Material Chemistry (MOE), School of Chemistry and Materials Science, Heilongjiang University, Harbin 150080, P.R. China E-mail: yanpf@vip.sina.com

b. State Key Laboratory of Rare Earth Resource Utilization, Changchun Institute of Applied Chemistry, Chinese Academy of Sciences, Changchun 130022, P.R. China. Email: tang@ciac.ac.cn

## Synthesis of N-methyl-4, 4'-diacetyldiphenylamine (MDA)

A 100-mL round-bottomed Schlenk flask was charged with anhydrous  $\text{AlCl}_3$  (1.82 g, 13.6 mmol) and dry dichloromethane (50 ml), and acetyl chloride (1.07 g, 13.6 mmol), resulting in a yellow transparent solution. A dry dichloromethane solution of N-methyl-phenylaniline (1.00 g, 5.46 mmol) was added dropwise to the above solution at  $-20\text{ }^\circ\text{C}$ . After kept 12 hours at room temperature, the resulting mixture was poured into 50mL ice-water and alkalized to  $\text{pH}=7$  using the aqueous solution of NaOH. The resulting organic layer was dehydrated by anhydrous sodium sulfate about 5 hours and then filtered. The crude product was chromatographed with petroleum ether/ethyl acetate (v/v, 5/1), and then the white product of V-shaped MDA was dried in vacuum (0.93 g, 64 wt%). Anal. Calc. for  $\text{C}_{17}\text{H}_{17}\text{NO}_2$  (267.32): C, 76.38; H, 6.41; N, 5.24 wt%. Found: C, 76.37; H, 6.40 N, 5.24 wt%. IR (KBr,  $\text{cm}^{-1}$ ): 3446 (w), 1600 (s), 1590 (m), 1401 (m), 1363 (s), 1264 (s).  $^1\text{H}$  NMR (400 MHz, DMSO- $d_6$ ,  $25\text{ }^\circ\text{C}$ , TMS):  $\delta= 7.92$  (d,  $J = 8.77$  Hz, 4H),  $7.20$  (d,  $J = 8.77$  Hz, 4H),  $3.42$  ppm (s, 3H),  $2.52$  ppm (s, 6H). The  $^1\text{H}$  NMR spectrum of MDA was shown in Figure S1.

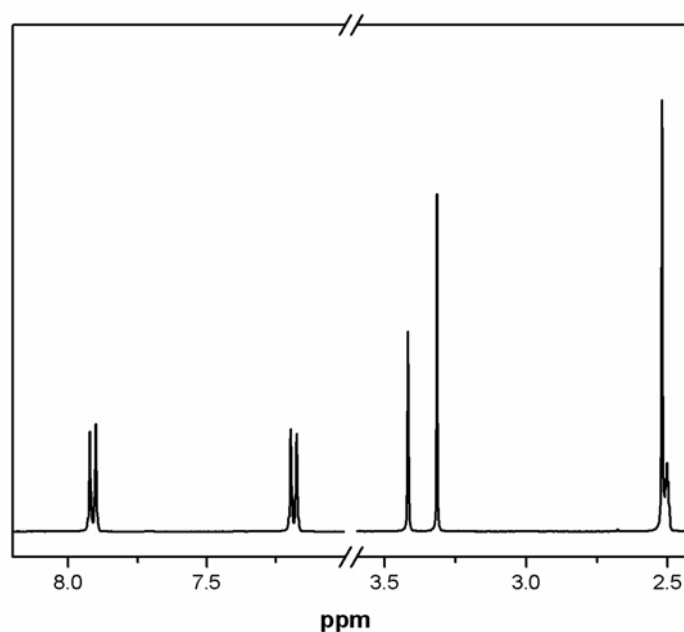


**Figure S1**  $^1\text{H}$  NMR spectrum of MDA

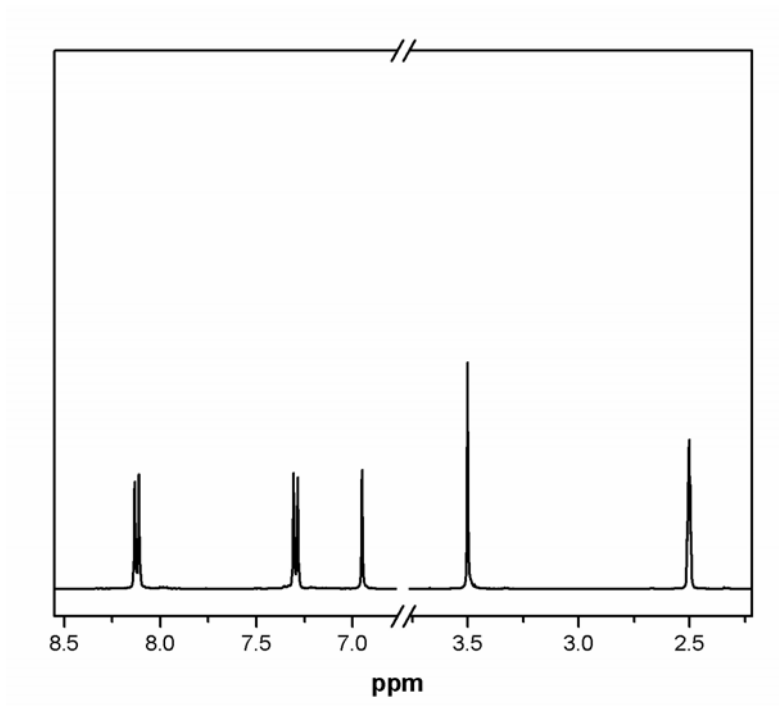


**Figure S2**  $^1\text{H}$  NMR spectrum of  $\text{H}_2\text{MBDA}$

## Structure determination

Suitable single crystals of **1**, **2** and MDA were selected for single crystal X-ray diffraction analysis. Diffraction intensity data were collected on an Oxford Diffraction Xcalibur Eos diffractometer with graphite-monochromated Mo K $\alpha$  radiation ( $\lambda = 0.71073 \text{ \AA}$ ). All data were collected at a temperature of 150 K. The structures were solved by the direct methods and refined on  $F^2$  by full-matrix least-squares using the SHELXTL-97 program.<sup>[1]</sup> The Ln<sup>3+</sup> ions were easily located and then non-hydrogen atoms (Cl, F, O, N and C) were placed from the subsequent Fourier-difference maps. In the case of **1**, Cl2 ion is located on a twofold axis and one Et<sub>3</sub>NH molecule is disordered with N(9) atom lied on a twofold axis as well. A summary for data collection and refinements were given in Table S1. CCDC: 1054122-4 contained the supplementary crystallographic data for this paper. These data could be obtained free of charge from the Cambridge Crystallographic Data Centre via [www.ccdc.cam.ac.uk/data\\_request/cif](http://www.ccdc.cam.ac.uk/data_request/cif).

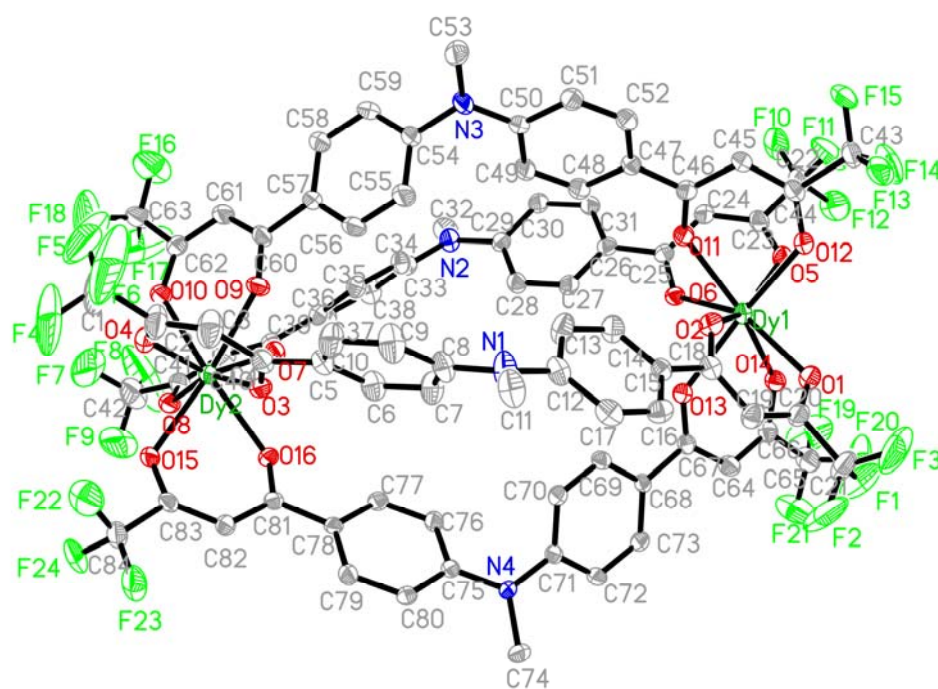


**Figure S3** ORTEP plot of **1**. The thermal ellipsoids are given at 50% probability (H atoms and guest species have been omitted for clarity).

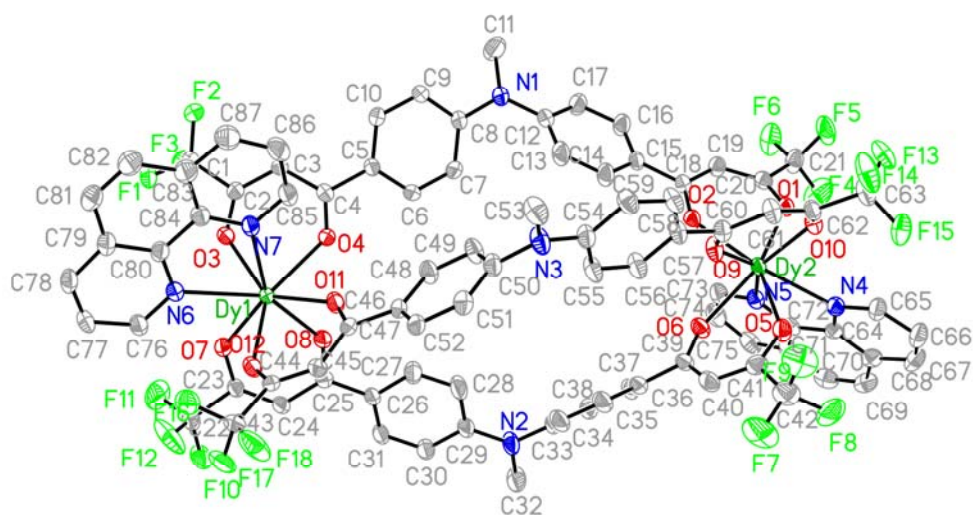


**Figure S4** ORTEP plot of **2**. The thermal ellipsoids are given at 50% probability (H atoms and guest species have been omitted for clarity).

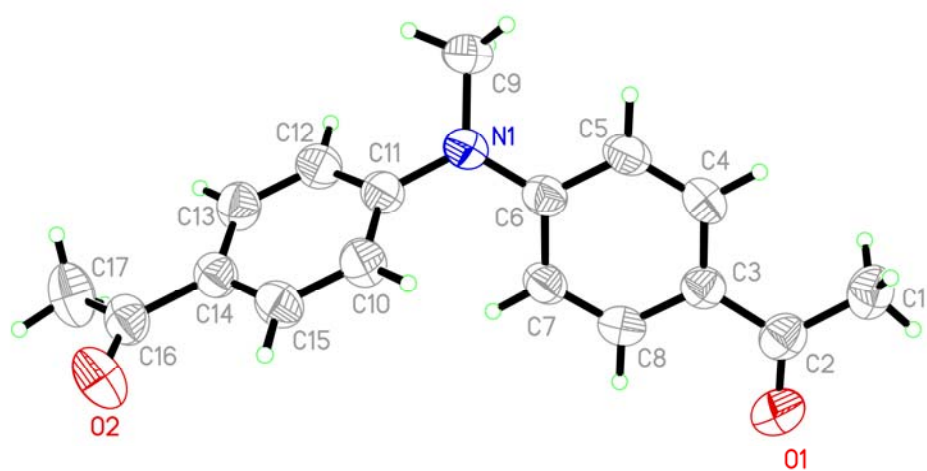


**Figure S5** ORTEP plot of V-shaped MDA. The thermal ellipsoids are given at 50% probability.

**Table S1** Crystal data and structural refinement for **1**, **2** and MDA.

Code	<b>1</b>	<b>2</b>	MDA
formula	C <sub>116</sub> H <sub>130</sub> Cl <sub>1.5</sub> Dy <sub>2</sub> F <sub>24</sub> N <sub>9.5</sub> O <sub>18</sub>	C <sub>95</sub> H <sub>72.5</sub> Dy <sub>2</sub> F <sub>18</sub> N <sub>7.5</sub> O <sub>14</sub>	C <sub>17</sub> H <sub>17</sub> N <sub>2</sub> O <sub>2</sub>
Mr	2779.47	2210.10	267.32
color	Colorless	Colorless	Colorless
crystal system	Monoclinic	Triclinic	Triclinic
space group	<i>C2/c</i>	<i>P</i> -1	<i>P</i> -1
Temperature (K)	150	150	150
<i>a</i> (Å)	45.2139(5)	12.1694(4)	8.2376(6)
<i>b</i> (Å)	20.4624(2)	19.7909(5)	8.5362(7)
<i>c</i> (Å)	28.0974(3)	21.6427(6)	10.4219(9)
$\alpha$ (deg)	90	66.933(3)	94.615(7)
$\beta$ (deg)	100.5900(12)	75.128(3)	98.690(7)
$\gamma$ (deg)	90	87.379(2)	99.967(7)
<i>V</i> (Å <sup>3</sup> )	25552.4(5)	4626.3(2)	709.21(10)
<i>Z</i>	8	2	2
$\rho$ (g cm <sup>-3</sup> )	1.445	1.587	1.252
$\mu$ (mm <sup>-1</sup> )	1.291	1.706	0.082
<i>F</i> (000)	11280	2202	2884
Reflections collected/unique	51469 / 27766	41308 / 20844	5518 / 3204
<i>R</i> <sub>int</sub>	0.0207	0.0236	0.0143
<i>R</i> <sub>1</sub> , [ <i>I</i> > 2 $\sigma$ ( <i>I</i> )]	0.0593	0.0338	0.0476
<i>wR</i> <sub>2</sub> , [ <i>I</i> > 2 $\sigma$ ( <i>I</i> )]	0.1665	0.0849	0.1089
<i>R</i> <sub>1</sub> , (all data)	0.0742	0.0432	0.0739
<i>wR</i> <sub>2</sub> , (all data)	0.1802	0.0906	0.1295
GOF on <i>F</i> <sup>2</sup>	1.028	1.042	1.031

Table S2 Selected bond lengths (Å) for **1** and **2**.

<b>1</b>			
Dy1–O11	2.359(4)	Dy1–O5	2.389(4)
Dy1–O6	2.385(4)	Dy1–O2	2.408(4)
Dy1–O12	2.376(4)	Dy1–O1	2.433(4)
Dy1–O13	2.364(4)	Dy1–O14	2.409(4)
Dy2–O3	2.367(4)	Dy2–O9	2.399(4)
Dy2–O4	2.372(4)	Dy2–O15	2.400(4)
Dy2–O7	2.373(4)	Dy2–O8	2.410(4)
Dy2–O16	2.386(4)	Dy2–O10	2.412(4)

<b>2</b>			
Dy1–O8	2.277(2)	Dy2–O10	2.311(2)
Dy1–O3	2.300(2)	Dy2–O9	2.313(2)
Dy1–O7	2.303(2)	Dy2–O2	2.316(2)
Dy1–O12	2.327(2)	Dy2–O1	2.320(2)
Dy1–O11	2.330(2)	Dy2–O6	2.330(2)
Dy1–O4	2.374(2)	Dy2–O5	2.351(2)
Dy1–N7	2.573(3)	Dy2–N4	2.532(3)
Dy1–N6	2.573(3)	Dy2–N5	2.557(3)



**Table S3** Selected C–H...F and F...F interactions in **1**.

C–H...F interactions	Distances (Å)	C–H...F interactions	Distances (Å)
C3–H3A...F6	2.729(10)	C53–H53A...F9_#1	3.307(10)
C115–H11H...F18	3.11(2)	C53–H53B...F2_#2	3.414(10)
C117–H11S...F18_#3	3.22(3)	C61–H61A...F16	2.727(8)
C19–H19A...F2	2.736(9)	C64–H64A...F21	2.728(8)
C24–H24A...F10	2.726(8)	C82–H82A...F23	2.734(7)
C40–H40A...F8	2.704(8)	C45–H45A...F15	2.720(7)
F...F interactions	Distances (Å)	F...F interactions	Distances (Å)
F1...F20	3.088(8)	F14...F11	3.031(7)
F10...F17_#4	3.109(8)	F17...F10_#4	3.109(8)
F11...F14	3.031(7)	F13...F23_#2	2.937(6)

Symmetry code used to generate the equivalent atoms: #1: x,-y,-1/2+z; #2: 1/2-x,1/2+y,1/2-z; #3: 1-x,y,3/2-z; #4: 1/2-x,1/2-y,1-z.

**Table S4** Selected C–H...F and F...F interactions in **2**.

C–H...F interactions	Distances (Å)	C–H...F interactions	Distances (Å)
C3–H3A...F2	2.750(4)	C40–H40A...F7	2.730(5)
C3–H3A...F18_#2	3.448(5)	C45–H45A...F18	2.738(5)
C19–H19A...F6	2.708(4)	C61–H61A...F14	2.733(5)
C24–H24A...F10	2.762(4)	C67–H67A...F3_#3	3.142(5)
C32–H32B...F17_#4	3.337(4)		
F...F interactions	Distances (Å)	F...F interactions	Distances (Å)
F2...F17_#2	3.009(3)	F5...F8_#2	3.015(4)
F2...F18_#2	2.942(4)	F6...F11_#1	3.098(4)
F11...F6_#1	3.098(4)		

Symmetry code used to generate the equivalent atoms: #1: 1-x, 1-y, -z; #2: -1+x, y, z; #3: 1+x, 1+y, -1+z; #4: 2-x, 1-y, -z;

**Table S5** The (Ph)C–N–C(Ph) bond angles in the ligand, and the dihedral angles of the two phenyl groups in the same ligand.

	1				2			MDA
Code	N1	N2	N3	N4	N1	N2	N3	N1
The (Ph)C–N–C(Ph) bond angles in the ligand containing <i>Nn</i> atom (deg)	120.9(5)	120.6(5)	120.7(5)	121.2(4)	122.6(3)	122.3(3)	121.6(3)	121.7(1)
The dihedral angles of the two phenyl groups bridging by <i>Nn</i> (deg)	62.(2)	56.6(2)	66.4(2)	55.1(2)	51.8(10)	54.7(1)	60.3(1)	61.7(5)

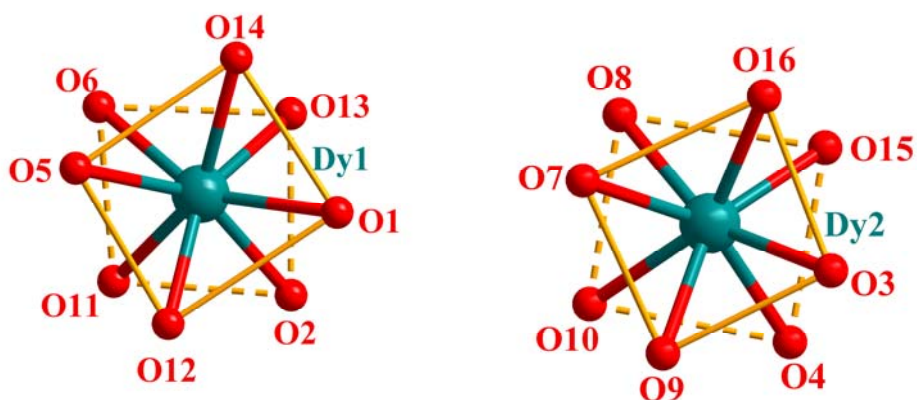


**Figure S6** The coordination geometries of Dy<sup>3+</sup> ions in **1**.

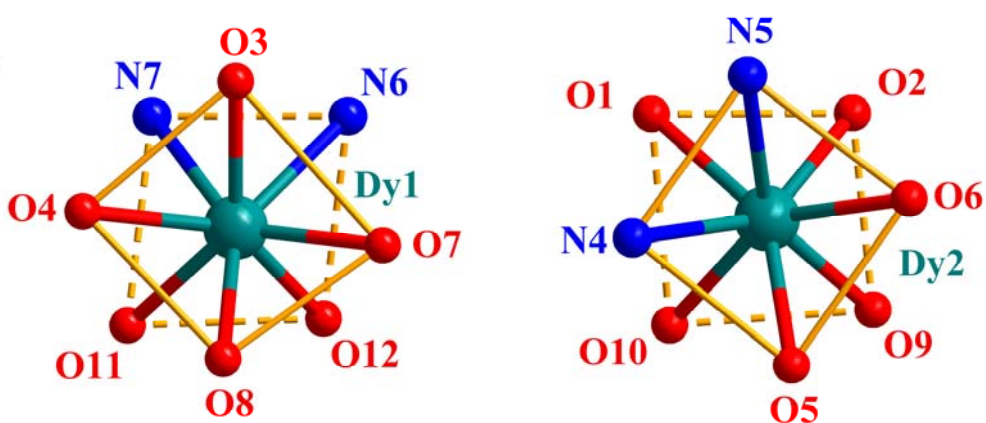


**Figure S7** The coordination geometries of Dy<sup>3+</sup> ions in **2**.

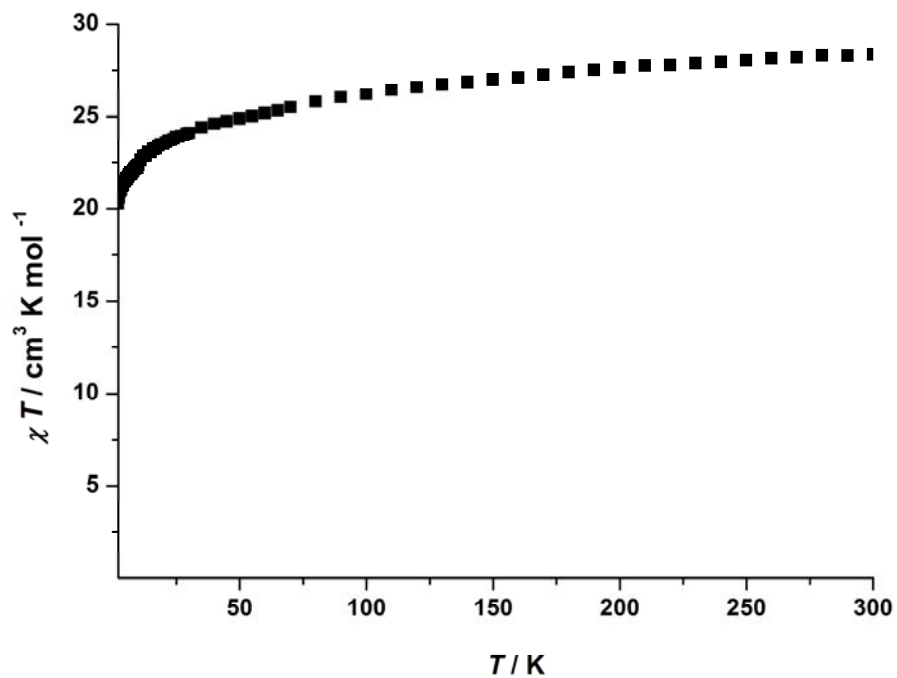


**Figure S8** Plot of  $\chi T$  vs  $T$  for **1** in an applied dc field of 500 Oe in the temperature range of 1.8-300 K.

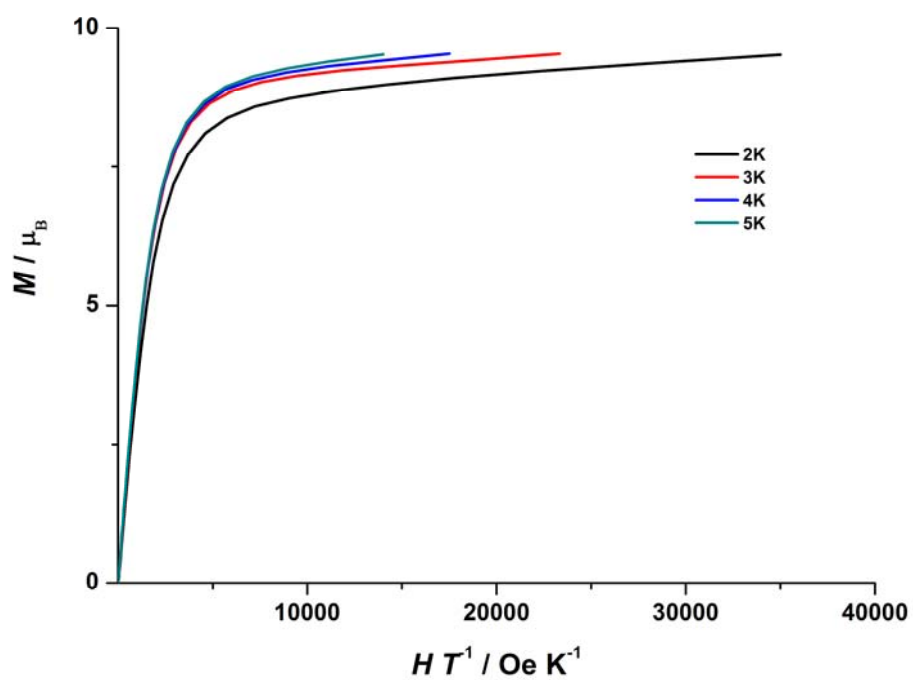


**Figure S9** Magnetization as a function of  $H/T$  for **1**.

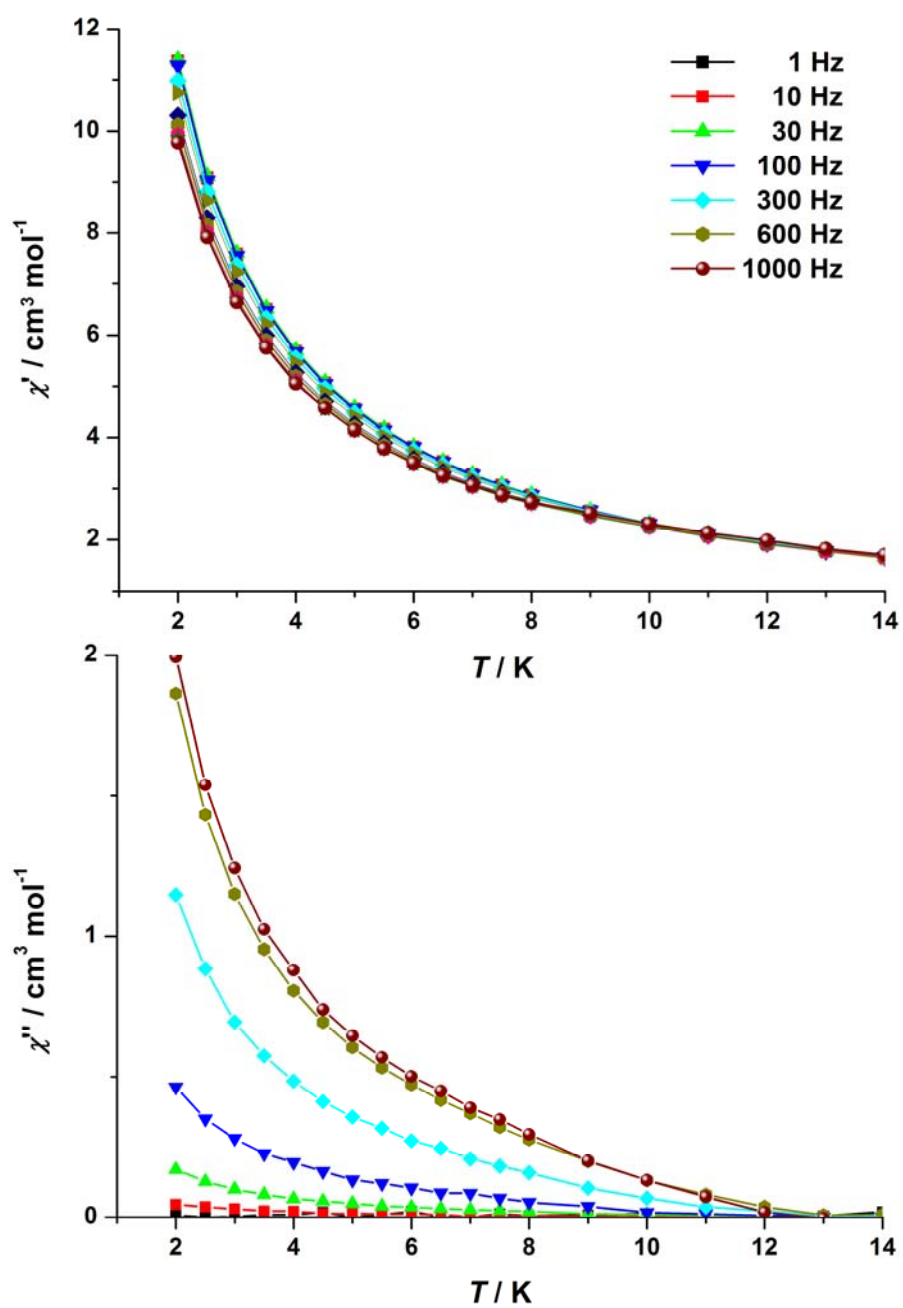


**Figure S10** Temperature dependence of the in-phase ( $\chi'$ , top) and the out-of-phase ( $\chi''$ , bottom) ac susceptibility from 2 to 14 K under zero dc field for **1**.

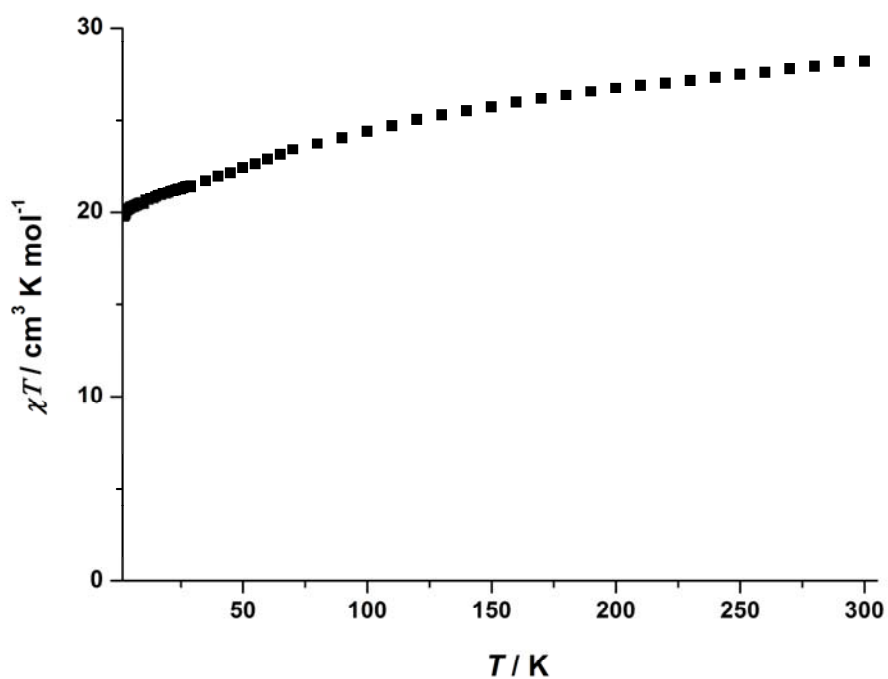


**Figure S11** Plot of  $\chi T$  vs  $T$  for **2** in an applied dc field of 500 Oe in the temperature range of 1.8-300 K.

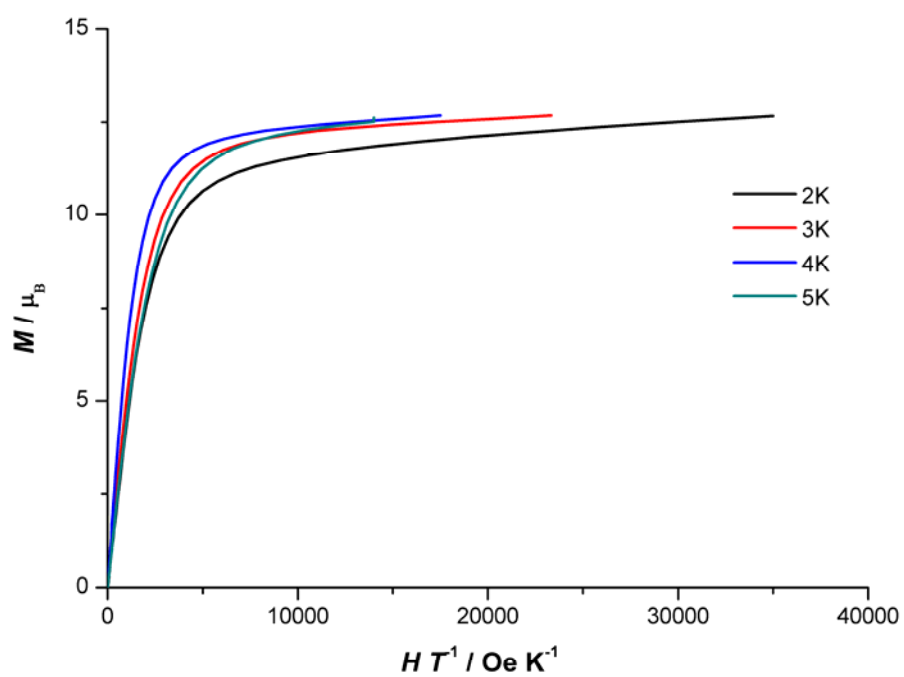


**Figure S12** Magnetization as a function of  $H/T$  for **2**.

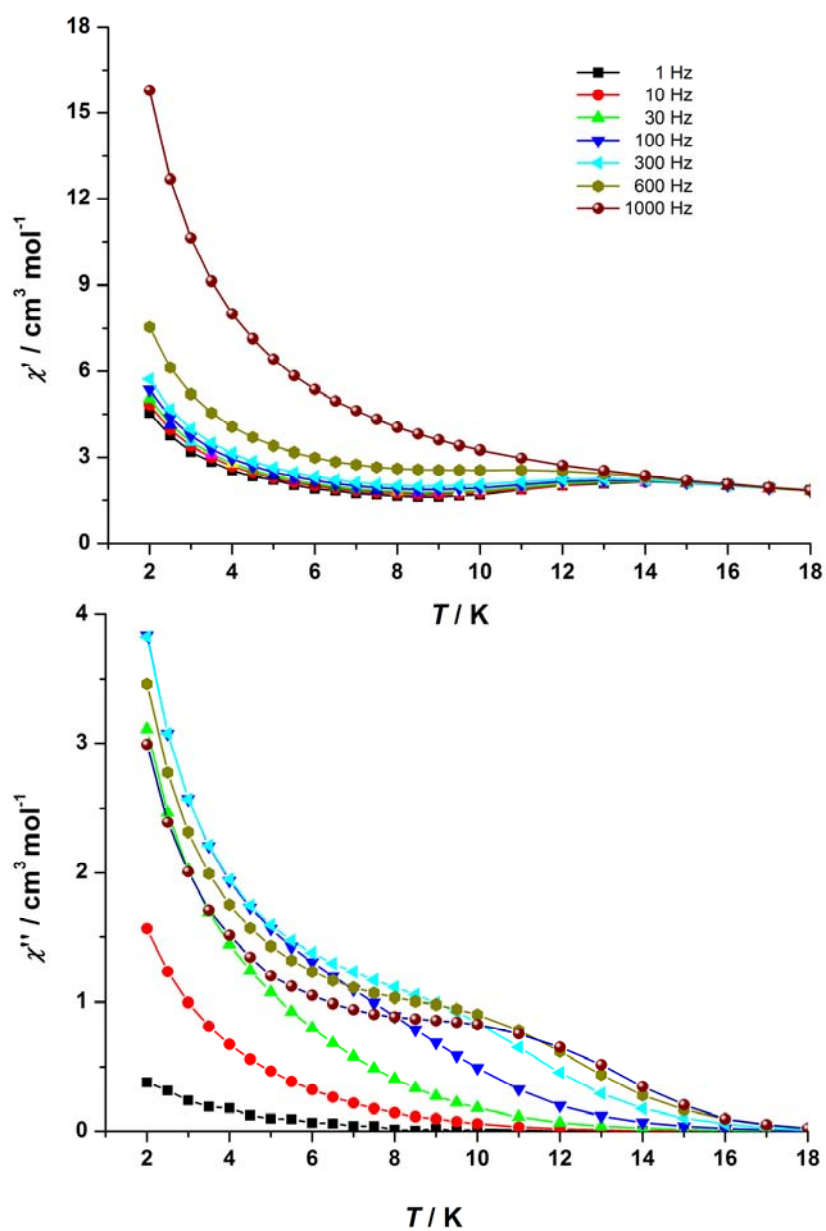


**Figure S13** Temperature dependence of the in-phase ( $\chi'$ , top) and the out-of-phase ( $\chi''$ , bottom) ac susceptibility from 2 to 18 K under zero dc field for **2**.

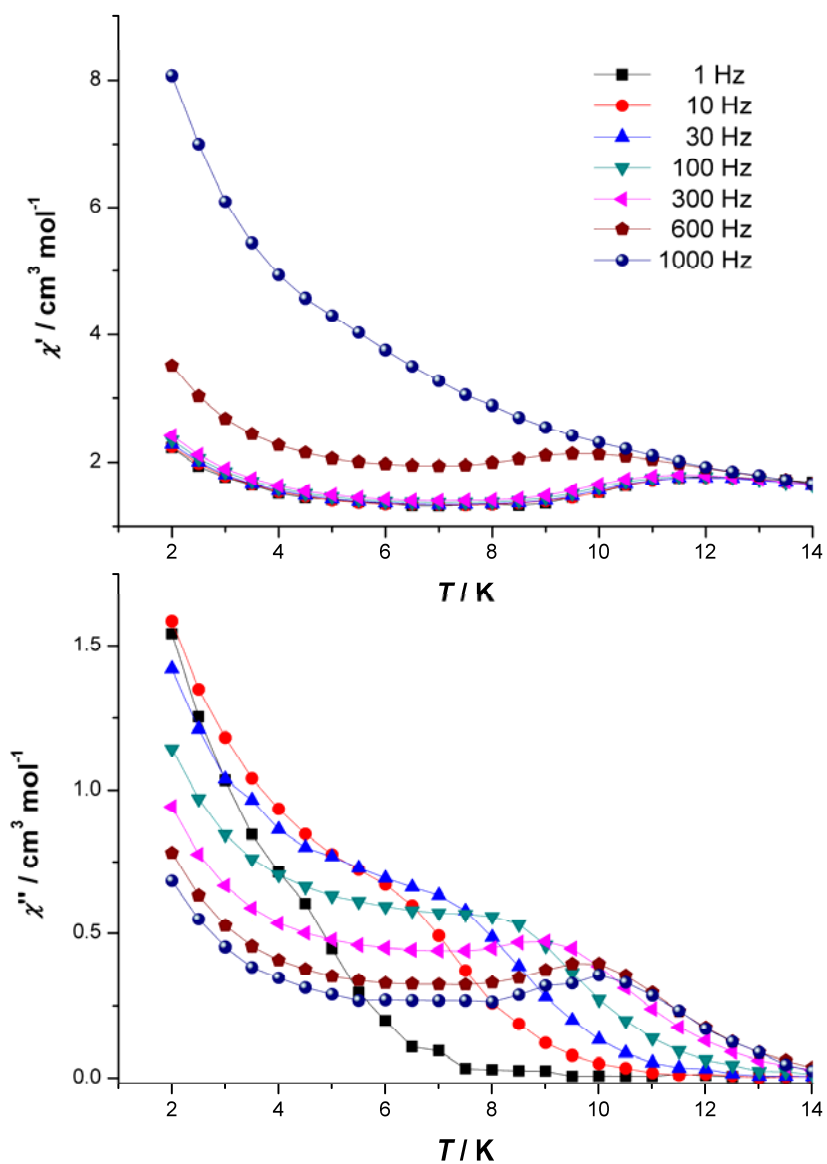


**Figure S14** Frequency dependence of the in-phase ( $\chi'$ , top) and out-of-phase ( $\chi''$ , bottom) ac susceptibility from 2 to 14 K under an applied field of 2000 Oe for **1**.



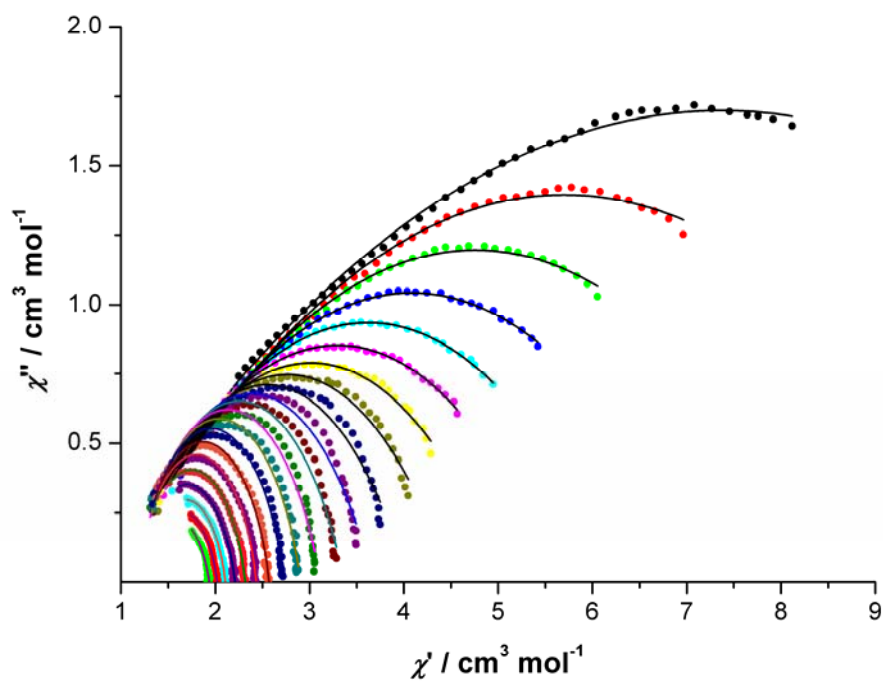


**Figure S15** Cole-Cole plots using the ac susceptibility data of **1** (2-12K, 0.5K interval).

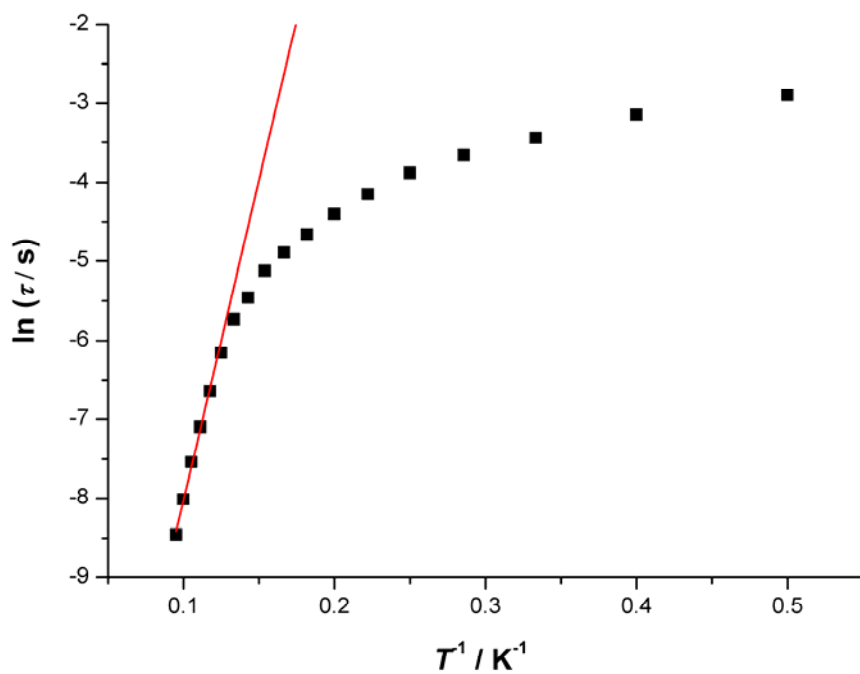


**Figure S16** The Relaxation time is plotted as  $\ln(\tau)$  vs  $T^{-1}$  for **1** under an applied field of 2000 Oe.

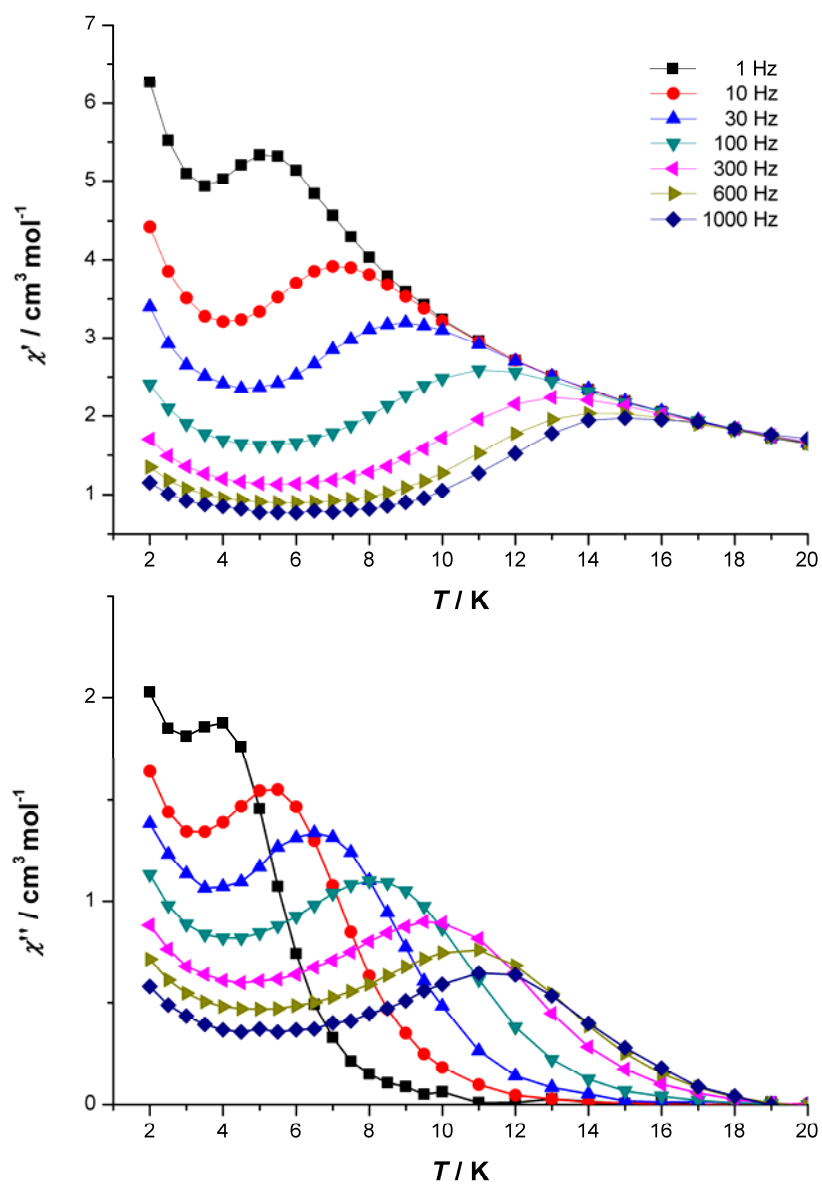


**Figure S17** Frequency dependence of the in-phase ( $\chi'$ , top) and out-of-phase ( $\chi''$ , bottom) ac susceptibility from 2 to 20 K under an applied field of 2000 Oe for **2**.

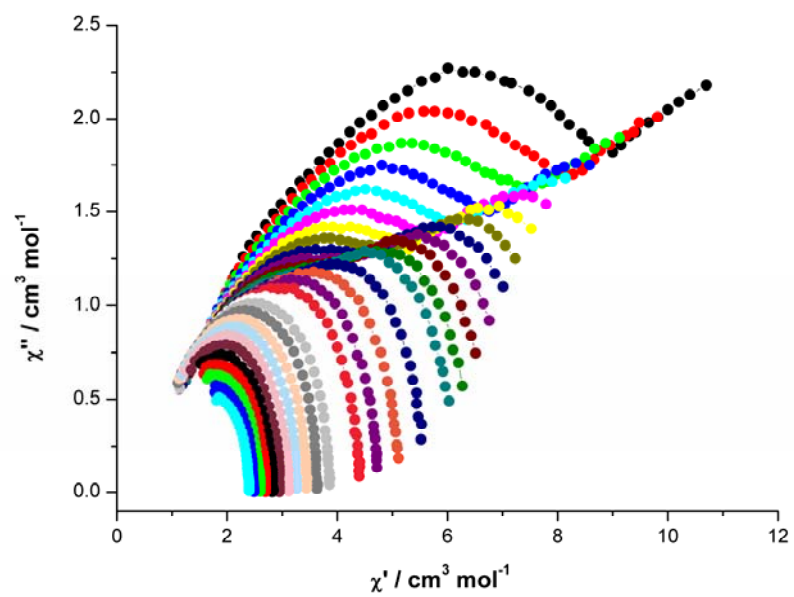


**Figure S18** Cole-Cole plots using the ac susceptibility data of **2** under an applied field of 2000 Oe (2-13K, 0.5K interval).

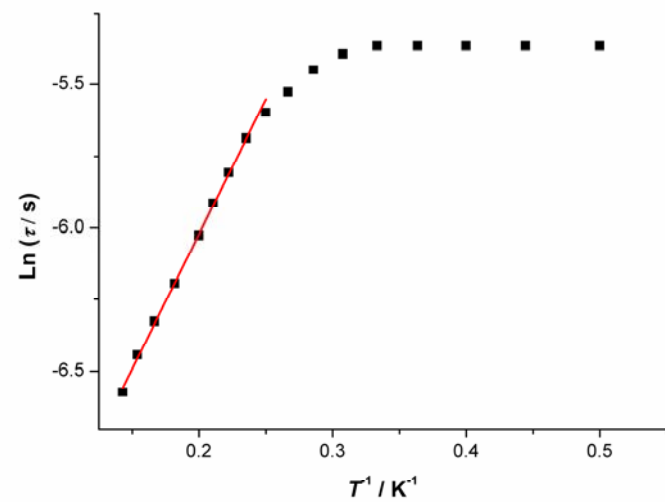
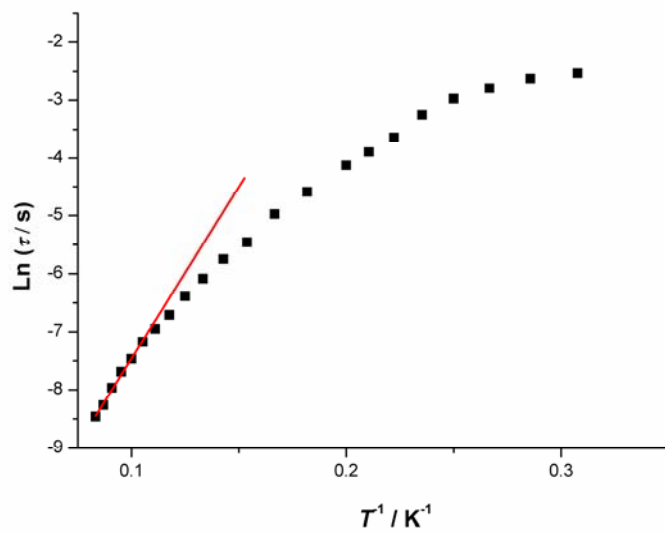


**Figure S19** The Relaxation times are plotted as  $\ln(\tau)$  vs  $T^{-1}$  for **2** under an applied field of 2000 Oe.

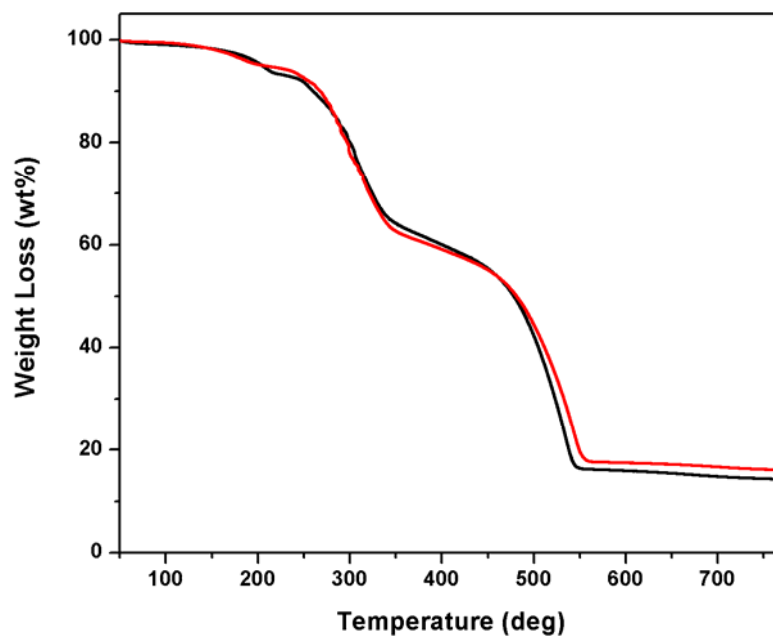


**Figure S20** Thermogravimetric curves for the precipitate of **1** (red line: precipitate washed with deionized water; black line: unwashed precipitate).

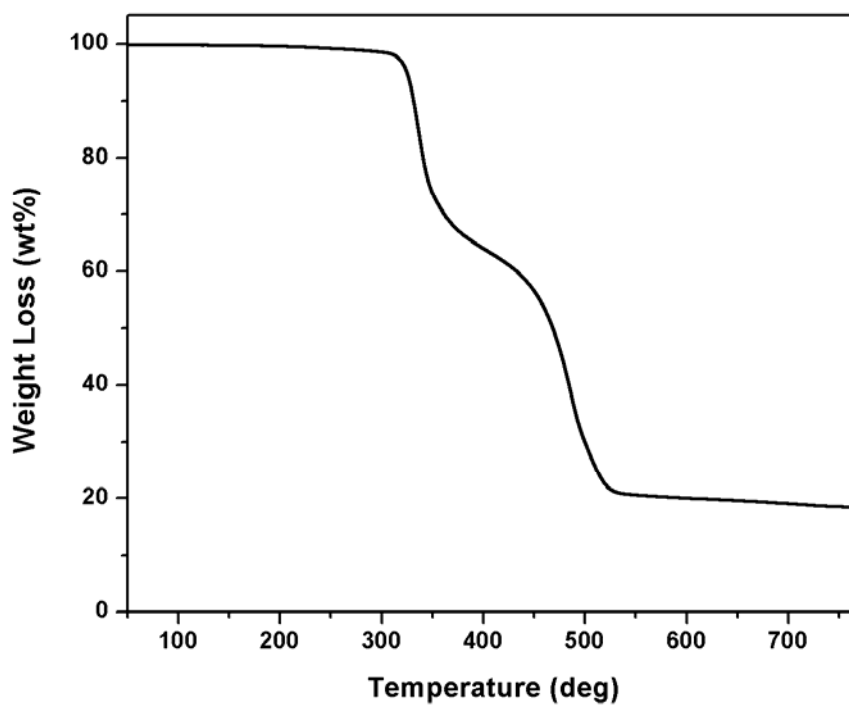


**Figure S21** Thermogravimetric curve for the precipitate of **2**.

Single crystal analysis indicates the existence of triethylammonium chloride in **1** and the thermogravimetric analysis is carried out on the as-synthesized precipitate of **1** (Fig. S20). A total weight loss of 85.74 wt% is found, which is lower than the expected value 84.19 wt% for the empirical formula  $[\text{C}_6\text{H}_{16}\text{N}]_2[\text{Dy}_2(\text{MBDA})_4]$ . It is supposed that the impurity of triethylammonium chloride might be involved in the as-synthesized precipitate of **1**. The precipitate is therefore washed with deionized water and dried under vacuum. The thermogravimetric analysis reveals a total weight loss of 83.91 wt% in accordance with the calculated value 84.19 wt%. In the first stage, a weight loss of 4.42 wt% (calcd. 4.28 wt%) is observed, owing to the removal of one triethylamine. In case of the unwashed precipitate, the weight loss of 6.27 wt% is ascribed to the removal of triethylammonium chloride (1.99 wt%) and one triethylamine. However, the subsequent decomposition might be a continuous process that it is hard to distinguish the removal of each ligand and second trimethylamine, respectively. The empirical formula of the unwashed precipitate is calculated as  $[\text{C}_6\text{H}_{16}\text{N}]_2[\text{Dy}_2(\text{MBDA})_4] \cdot 0.35(\text{C}_6\text{H}_{15}\text{N} \cdot \text{HCl})$ . The impurity of triethylammonium chloride in the unwashed precipitate is expected to result from excessive triethylamine and chloride anion. Fortunately, it might have been helpful to the crystallization of **1**. The thermogravimetric curve of the powder of **2** indicates a total weight loss of 81.65 wt% in good agreement with the calculated value 81.87 wt% (Fig. S21).

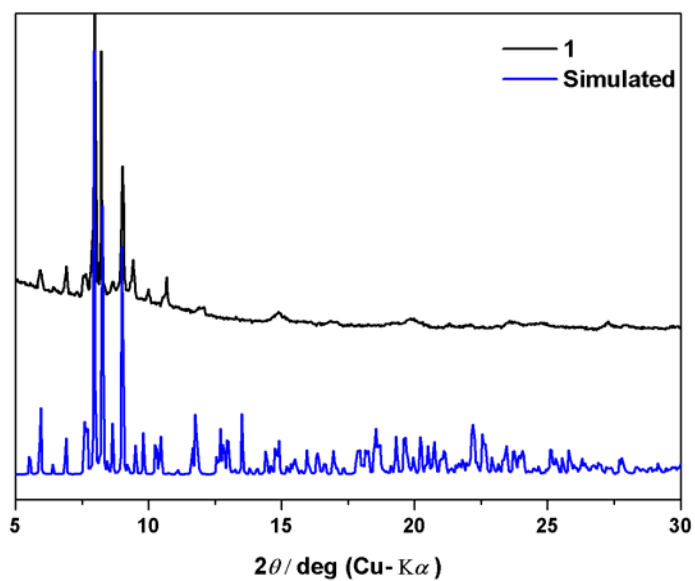


**Figure S22** Simulated and experimental PXRD patterns of **1**.

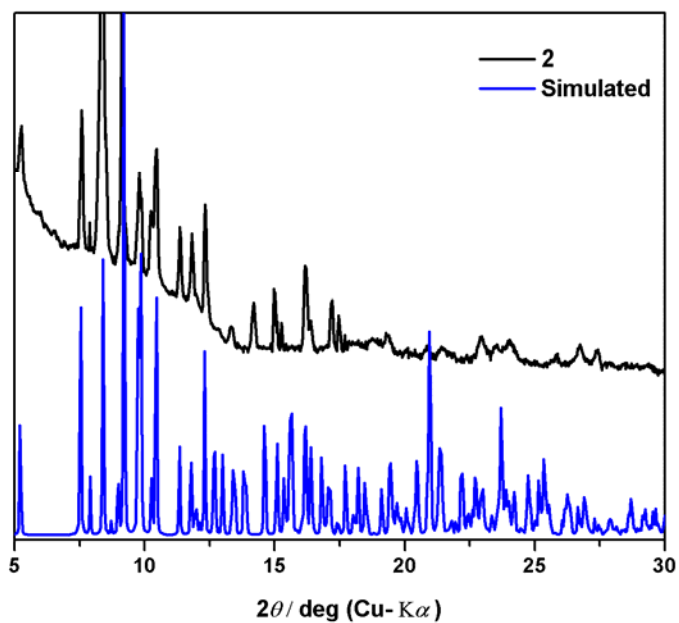


**Figure S23** Simulated and experimental PXRD patterns of **2**.

The crystals of **1** and **2** are supposed to be sensitive to the air that the crystals are deteriorated on desolvation, when they are exposed in air.

**References:**

- [1] G. M. Sheldrick, SHELXL-97, Program for X-ray Crystal Structure Refinement, University of Göttingen, Göttingen, Germany, 1997.
- [2] D. Casanova, M. Llunel, P. Alemany, S. Alvarez, Chem.–Eur. J. 2005, 11, 1479.